RHEUMATOID ARTHRITIS

Inflammatory but not mitogenic contexts prime synovial fibroblasts for compensatory signaling responses to p38 inhibition

Douglas S. Jones,[1,2] Anne P. Jenney,[2] Brian A. Joughin,[1,3] Peter K. Sorger,[2] Douglas A. Lauffenburger[1,3]*

Rheumatoid arthritis (RA) is a chronic inflammatory disorder that causes joint pain, swelling, and loss of function. Development of effective new drugs has proven challenging in part because of the complexities and interconnected nature of intracellular signaling networks that complicate the effects of pharmacological interventions. We characterized the kinase signaling pathways that are activated in RA and evaluated the multivariate effects of targeted inhibitors. Synovial fluids from RA patients activated the kinase signaling pathways JAK, JNK, p38, and MEK in synovial fibroblasts (SFs), a stromal cell type that promotes RA progression. Kinase inhibitors enhanced signaling of "off-target" pathways in a manner dependent on stimulatory context. Inhibitors of p38, which have been widely explored in clinical trials for RA, resulted in undesirable increases in nuclear factor κB (NF-κB), JNK, and MEK signaling in SFs in inflammatory, but not mitogenic, contexts. This was mediated by the transcription factor CREB, which functions in part within a negative feedback loop in MAPK signaling. CREB activation was induced predominately by p38 in response to inflammatory stimuli, but by MEK in response to mitogenic stimuli; hence, the effects of drugs targeting p38 or MEK were markedly different in SFs cultured under mitogenic or inflammatory conditions. Together, these findings illustrate how stimulatory context can alter dominance in pathway cross-talk even for a fixed network topology, thereby providing a rationale for why p38 inhibitors deliver limited benefits in RA and demonstrating the need for careful consideration of p38-targeted drugs in inflammation-related disorders.

INTRODUCTION

Rheumatoid arthritis (RA) is an autoimmune disease characterized by inflammation and swelling of synovial joints, systemic complications, and significant morbidity and mortality (1–3). At the cellular level, autoantibodies and autoreactive T cells are believed to be responsible for the initiation of RA (4, 5), although increasing evidence suggests that synovial fibroblasts (SFs)—the resident fibroblast-like cells of the synovial membrane—play a critical role in perpetuating disease (6, 7). In healthy tissue, SFs form a one- to two-cell-thick layer at the lining of the synovium, function to maintain the synovial membrane architecture, and produce lubricating molecules for the joint (8, 9). In RA, however, SFs have been described as transformed cells, in which they display morphologic features similar to cancer cells such as hyperplasia and resistance to apoptosis (6, 10). They also secrete various inflammatory cytokines and matrix-degrading proteases (9, 11), including many of the most abundant cytokines in synovial fluids of RA patients (12). In addition, SFs from RA patients (RA SFs), but not SFs from normal or osteoarthritis (OA) patients, are capable of invading and degrading human cartilage in immunodeficient mouse models of RA (13–15). The activated SF phenotype persists for several passages ex vivo, but RA SFs eventually adopt a more quiescent state after a few weeks in culture. Exposure to inflammatory cytokines such as interleukin-1 (IL-1) or tumor necrosis factor–α (TNFα) can restore the activated state, suggesting that SF activation in RA is dynamic and dependent on inflammatory factors in the RA joint (10).

Biologic drugs targeting cytokines such as TNFα, IL-6, and IL-1, which mediate proinflammatory communication among the cells of the RA synovium, have improved disease management (16–20). However, resistance to treatment is a significant challenge, and fewer than 50% of patients remain in remission for 1 year (21). The U.S. Food and Drug Administration's (FDA) approval of tofacitinib (Xeljanz), a small molecule inhibitor of the Janus kinases (JAKs), for RA demonstrates the therapeutic potential for targeting the kinases that regulate cytokine signaling and has brought promise for effective new therapies (22). However, drugs targeting other kinase pathways such as p38, mitogen-activated protein kinase (MAPK)/extracellular signal–regulated kinase (ERK) kinase (MEK), and spleen tyrosine kinase (Syk) have been met with limited success in clinical trials (23, 24). In particular, p38 inhibitors received considerable interest from the pharmaceutical industry for their ability to reduce inflammatory cytokine secretion in preclinical models, but they failed to show meaningful efficacy in clinical trials (23, 25). Drugs targeting p38 are no longer being developed for RA, but remain of interest for other inflammation-related disorders (25). Much of the negative clinical trial data for RA has not been published publicly (25), which limits the ability to both fully understand the reasons for their lack of clinical efficacy and apply this learning to ongoing exploration of p38 inhibition in other inflammatory disorders. Their failure in RA, however, is thought to be based at least in part on an incomplete understanding of the effects of kinase-targeted drugs on complex, interconnected intracellular signaling networks, particularly as influenced by the complex inflammatory microenvironment in RA.

Here, we combined high-throughput experimentation and data-driven modeling to explore inflammatory signaling responses of SFs and to evaluate the multivariate effects of specific kinase inhibitors on these inflammatory responses. Given the limited quantities of RA

[1]Department of Biological Engineering, Massachusetts Institute of Technology, Cambridge, MA 02139, USA. [2]Laboratory of Systems Pharmacology, Library of Integrated Network-based Cellular Signatures Center, Harvard Medical School, Boston, MA 02115, USA. [3]Koch Institute for Integrative Cancer Biology, Massachusetts Institute of Technology, Cambridge, MA 02139, USA.
*Corresponding author. Email: lauffen@mit.edu

synovial fluids that we could obtain from an individual patient, we first developed an understanding of the effects of recombinant cytokine stimuli and kinase-targeted drugs on inflammatory responses of SFs, and then conducted a series of focused studies using synovial fluids from RA patients. We found that RA synovial fluids potently activated multiple stress-activated and inflammatory signaling pathways in SFs, such as the JNK, p38, and JAK/signal transducer and activator of transcription (STAT) pathways. This response was consistent across SFs from healthy and RA tissues, suggesting that both normal and RA SFs are similarly capable of activation by inflammatory factors in the RA microenvironment. We also found that drugs targeting p38 significantly increased activation of pathways linked to RA progression specifically in the presence of inflammatory factors, such as TNFα and IL-1α, but not for the mitogenic stimulus epidermal growth factor (EGF). To identify such context dependencies from our large-scale data, it was necessary to control for the confounding effects of multiple simultaneous perturbations (such as combinations of stimulatory cytokines and kinase-targeted inhibitors) by incorporating information about the experimental design into our statistical modeling analyses. Together, our findings characterize pathways activated in SFs by the inflamed synovial environment, provide evidence that negative regulatory cross-talk by p38 limited the clinical benefit of targeting p38 for RA, and demonstrate the utility of a broad perturbational framework for providing insight into multivariate drug effects.

RESULTS

Characterization of signaling pathways activated in RA SFs

SFs from RA patients display uniquely aggressive properties that are not observed in cells from normal or OA donors (14, 15). To characterize pathways activated in RA, we measured the effects of disease-related inflammatory stimuli on intracellular signaling pathways believed to be involved in inflammatory cytokine signaling or SF biology (Fig. 1A) (7, 26, 27). Given their strong connection to RA, the stimuli included TNFα, IL-1α, and IL-6 (28, 29). We additionally included EGF as a stimulus due to its presence at high levels in the RA synovium (30) and as a positive control for the activation of phosphatidylinositol 3-kinase (PI3K)/AKT and MEK/ERK pathways, two canonical pathways of the EGF receptor. To compare potential differences in responsiveness between normal and RA SFs, we evaluated responses of SFs from four healthy and four RA human tissues. The primary human SFs were propagated in culture and then individually exposed to the stimuli for 10 or 30 min. Cells were then fixed and immunostained to measure phosphorylation or nuclear localization of the intracellular signaling nodes using high-throughput immunofluorescence microscopy and image analysis (fig. S1 and table S1). Cells were exposed to stimuli in biological quadruplicate (biological duplicates within experiments conducted on two separate days) to result in a compendium of ~5000 data points quantifying the immediate-early signaling responses across multiple normal and RA SF samples (fig. S2 and, for SF sample information, table S2). Correlation of experimental replicates was generally high and consistent across SF samples and signaling nodes, indicating a high-quality data set (average Pearson correlation ≥0.75 across experimental replicates for 11 of 13 nodes; fig. S3). An exception to this was phosphorylated JNK (p-JNK), whose correlation between the two experiments varied across the SF samples (correlation ranged from 0.51 to 0.86, $\rho_{avg} = 0.69$; fig. S3). This may have been due to moderate anti–p-JNK antibody quality because p-c-Jun, a transcription

factor downstream of JNK, was tightly correlated across experiments for all SF samples ($\rho = 0.97 \pm 0.02$). The other exception was p-AKT ($\rho = 0.55 \pm 0.2$). Its poor correlation across experiments appeared to result from activation of AKT primarily only by EGF in this data set. This activation was additionally highly transient, peaking at 10 min and returning near to baseline levels by 30 min (fig. S2). Notably, these dynamics differed both from that of ERK activation, which was increased at both 10 and 30 min after EGF stimulation (fig. S2), and from AKT signaling in cancer cell lines exposed to EGF, which generally exhibit more sustained AKT activation through 90 min (31). Overall, we conclude that this is a high-quality data set for exploring SF activation in response to factors associated with RA.

To score pathways activated by each stimuli, we analyzed the data using multiple linear regression (MLR; figs. S4 and S5; see also Materials and Methods), a useful method for determining input-output relationships between perturbations and cellular responses (32). This resulted in MLR models for each SF donor sample and time point in which the MLR β coefficients represented a model of the effects of each stimulus on a given signaling node. More sophisticated analyses are possible, but previous studies have shown that MLR performs well for data such as ours (32, 33), and we found MLR to be an interpretable and statistically rigorous approach to score pathway activities across multiple donor samples and stimuli. The MLR β coefficients were consistent across donor samples, with 93.5% of inferred connections occurring in at least six of the eight SF donor samples. IL-6 was the only stimulus to consistently induce JAK/STAT pathway activity across multiple SF donor samples (Fig. 1B and fig. S5). TNFα, IL-1α, and EGF each activated the MAPK pathways MEK, p38, and JNK, whereas TNFα and IL-1α additionally activated the nuclear factor κB (NF-κB) pathway [Benjamini-Hochberg (34) false discovery rate (FDR; q_{BH}) < 0.01; Fig. 1B]. The p38 and JNK pathways are key "stress" pathways involved in responses to stress stimuli, including inflammatory cytokines. Consistent with this function, we found that activation of p38 and JNK signaling by EGF was much lower than that for TNFα or IL-1α (fig. S6). Notably, however, whereas activation of the MEK/ERK pathway, which is involved in cell proliferation and cell cycle progression, is usually low or absent for inflammatory stimuli as compared to mitogenic factors such as EGF (35), we found that maximal activation of the MEK/ERK pathway by TNFα and IL-1α approached similar levels to that of EGF (fig. S6).

To more broadly explore correlations among the measured signaling nodes, we visualized the β coefficients for each cytokine and SF sample in a reduced dimensional space using principal components analysis (PCA). The resulting PCA coefficients reflect the covariance of the measured signaling nodes across stimuli, time points, and SF samples and are consistent with our understanding of kinase signaling network architecture. For example, projections of components within the same canonical pathway are largely aligned [namely, JNK pathway: p-JNK and p-c-Jun; p38 pathway: p-p38, p-Hsp27 (phosphorylated heat shock protein 27), and p-MK2 (phosphorylated MAPK-activated protein kinase 2; also known as MAPKAPK2); and JAK/STAT pathway: p-STAT1 and p-STAT3], and the projection of the transcription factor FoxO3a (forkhead box O3) is approximately antiparallel to p-AKT and p-ERK, which is consistent with the negative regulation of FoxO3a by the PI3K/AKT and MEK/ERK pathways (Fig. 1C). For a given time point, the projection of p-CREB [phosphorylated cyclic adenosine monophosphate (cAMP) response element–binding protein] is largely orthogonal to that of p-ERK and p-p38 (Fig. 1C). This would typically suggest independence from the MEK/ERK and p38 pathways,
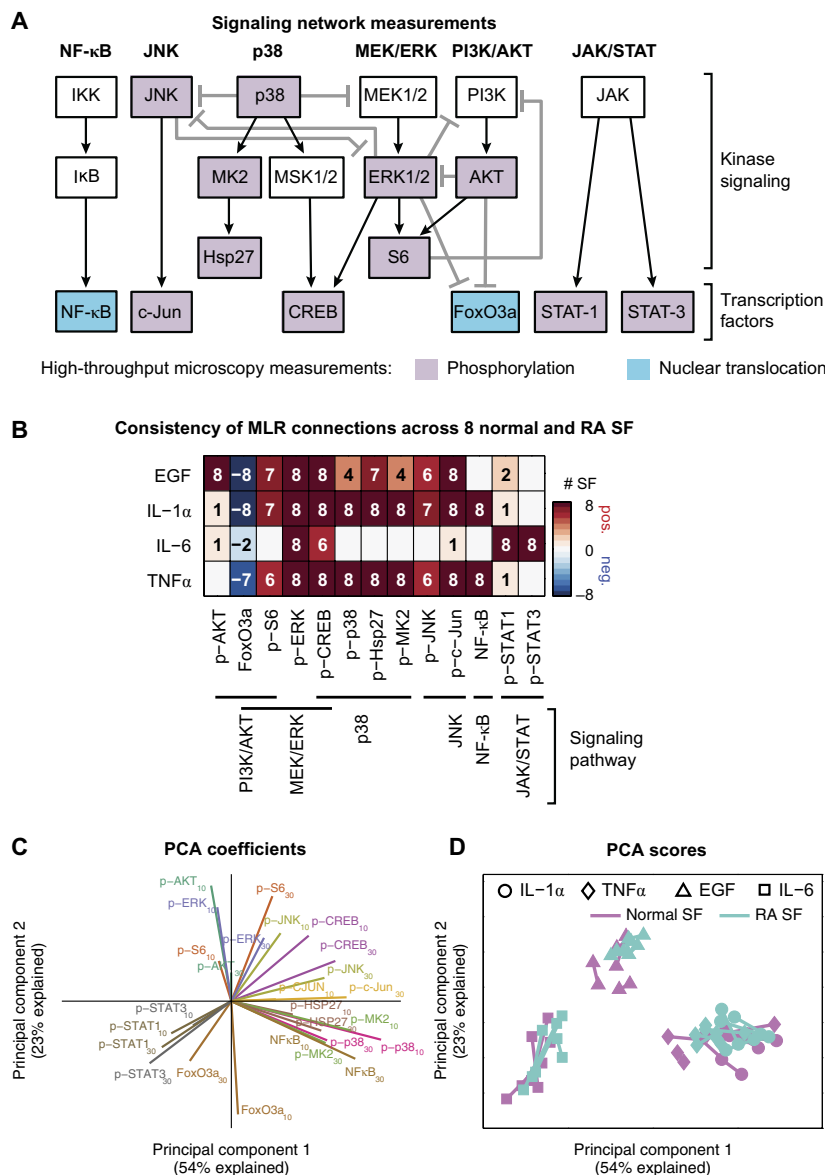
Fig. 1. Consistent responses of normal and RA SF to inflammatory cytokines. (**A**) Simplified signaling network topology showing measured nodes and their relevant canonical signaling pathways. Activation was evaluated after 10 and 30 min of stimulation with epidermal growth factor (EGF), interleukin-6 (IL-6), tumor necrosis factor–α (TNFα), or IL-1α (100 ng/ml each) in biological duplicate in four normal and four rheumatoid arthritis (RA) synovial fibroblast (SF) samples; a full experimental replicate was performed on separate days for a total of four replicates for each stimulus. (**B**) Summary of the activation of network proteins (columns) by the stimuli (rows) was categorized as positive or negative based on MLR β coefficients merged across experiments and time and counted across the eight SF samples (four normal and four RA). (**C** and **D**) Principal components analysis (PCA) of MLR β coefficients for the network proteins. PCA coefficients (C) for different time points of a given signaling protein are shown in the same color. PCA scores (D) for MLR coefficients for a given stimuli and SF sample in the two experimental replicates are connected by a line.

(Fig. 1A) and is also activated by EGF, TNFα, and IL-1α (Fig. 1B), which manifests as the p-CREB coefficients bisecting the p-ERK and p-p38 coefficients. Notably, the PCA scores of the MLR coefficients cluster according to stimulatory context, with no clear divergence between normal and RA SFs (Fig. 1D). Among individual stimuli, the eight SF samples also displayed consistent activation and dynamics between both normal and RA SFs (fig. S6). We conclude that the MLR networks (and the primary data from which they are derived) capture complex features of kinase signaling network architecture, which supports the utility of our perturbational approach for examining SF activation. In addition, for the stimuli examined here, stimulatory context plays a greater role in determining SF activation state than inherent differences between SF from normal and RA tissues.

Evaluation of multipathway effects of MAPK inhibitors

Inhibition of MEK, JNK, and p38 signaling has been explored previously for RA therapy (7, 23, 25). Although we found above that each of these pathways is strongly activated by TNFα and IL-1α in SF, clinical studies of drugs targeting these pathways have resulted in limited benefit. To explore whether potential signaling pathway cross-talk might limit the benefit of inhibitors targeting these pathways, we evaluated the multivariate effects of drugs targeting MAPK signaling in SFs. We first explored the effects of two specific p38 inhibitors [SB202190 (36) and PH-797804 (37)] on p38 and JNK signaling. Both p38 inhibitors not only reduced p38 pathway activity (as monitored by p-Hsp27) but also elevated JNK pathway activity in a dose-dependent manner (as monitored by p-c-Jun) specifically at a late time point (90 min after stimulation) but not at an early/intermediate time point (30 min after stimulation; Fig. 2, A to C). To systematize this analysis, we needed to incorporate context into our analytical framework. For example, in considering the opposite effects of the p38 inhibitor SB202190 on p-Hsp27 and p-c-Jun at the 90-min time point (Fig. 2B), one might expect that the data for these two signaling nodes are negatively correlated. Such a correlation, however, does not reach a level of statistical significance ($P = 0.087$; Fig. 2D) due to the confounding effect of IL-1α, which activates both nodes. As shown above, we can control for the effect of IL-1α on these signaling nodes using MLR by regressing the data for each signal against the presence or absence of
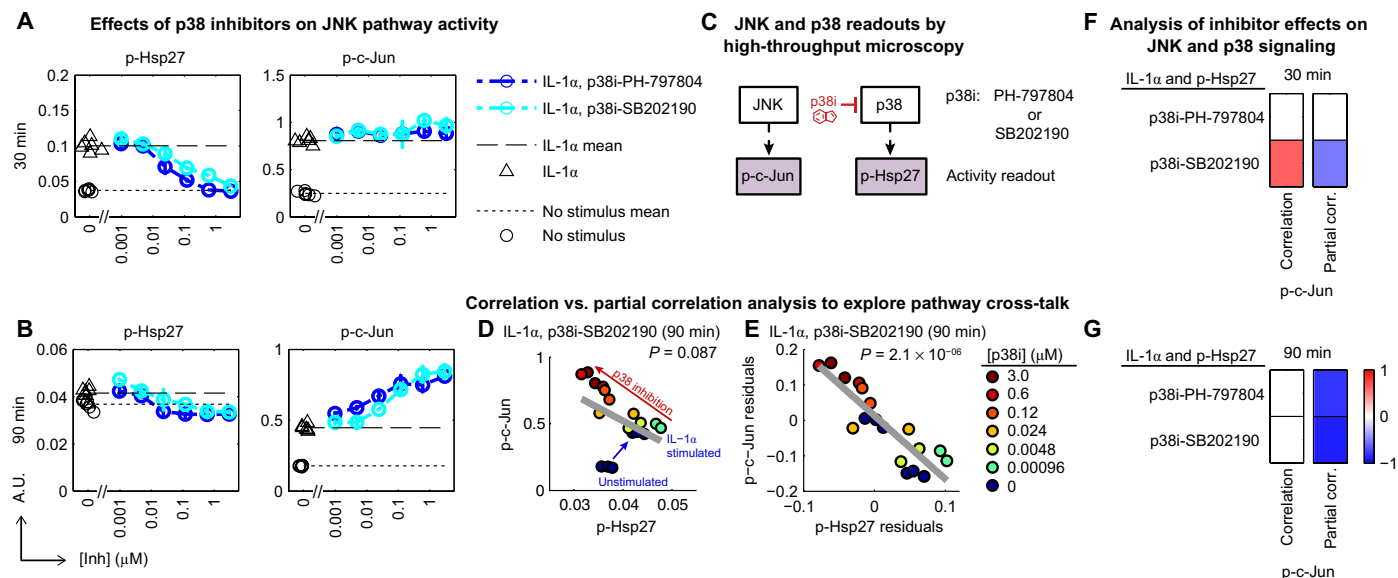
but a closer inspection suggests a more complicated interpretation. The strong activation of p-ERK by EGF at both 10 and 30 min post-stimulation results in the p-ERK coefficients projecting toward the EGF scores (compare in Fig. 1, C and D), whereas the strong activation of the p38 pathway by IL-1α and TNFα results in the p-p38 coefficients projecting toward the IL-1α and TNFα scores (compare in Fig. 1, C and D). CREB is regulated by the MEK and p38 pathways

Fig. 2. Enhancement of JNK signaling by p38 inhibition. (**A** to **C**) Perturbational strategy and dose-response data for evaluation of two specific p38 inhibitors on c-Jun and Hsp27 phosphorylation (and thus, activation) after 30 or 90 min of stimulation with IL-1α (100 ng/ml). Serial fivefold dilutions of inhibitor (0.00096 to 3 μM) were performed in biological duplicate in RA SF sample RA2159. Data are means ± SD. (**D**) Pearson correlation between p-Hsp27 and p-c-Jun for the 90-min time point and p38 inhibitor SB202190. (**E**) Partial correlation analysis of p-c-Jun and p-Hsp27: correlation between the p-c-Jun and p-Hsp27 residuals after controlling for the effect of IL-1α on p-Hsp27 and on p-c-Jun using multiple linear regression (MLR). (**F** and **G**) The correlation and partial correlation frameworks in (D) and (E) were applied to the data for both p38 inhibitors at the 30-min (F) or 90-min (G) time points. Partial correlations in (F) and (G), with $q_{BH} \geq 0.05$ were set to 0. A.U., arbitrary fluorescence units.

IL-1α. The unexplained effect of each signal (that is, the MLR model residuals) should contain information about the inhibitor, which represents an experimental perturbation that was deliberately unaccounted for in the model. Removal of the IL-1α dependency in this manner highlights the significant negative correlation between p-Hsp27 and p-c-Jun ($P = 2.1 \times 10^{-6}$; Fig. 2E). This analysis is referred to as partial correlation (*38*) because it analyzes the correlation between two variables (in this case, p-Hsp27 and p-c-Jun) that is not explained by a third variable (IL-1α stimulation). Applying this partial correlation analysis framework to the full data set (Fig. 2, A and B) revealed that this negative partial correlation is consistent for both p38 inhibitors (partial correlation at 90 min = −0.8 to −0.9; $P < 0.0001$), a relationship that is not detectable by traditional correlation analysis (Fig. 2, F and G). Thus, when evaluating relationships from multiperturbation experiments (for example, stimulus and inhibitor combinations), explicitly including aspects of the experimental design in the analytical framework can help control for effects of individual perturbations and uncover significant associations in the data.

To explore multipathway effects of inhibitors against each of the three MAPK pathways, we measured the effects of specific p38 (PH-797804), JNK (JNK-IN-8) (*39*), or MEK (PD184352) (*36, 40*) inhibitors on signaling in SFs after 90 min of incubation with IL-1α (Fig. 3A and, for additional inhibitor information, table S3). We selected phosphorylation of c-Jun, Hsp27, and ERK, which are downstream nodes of JNK, p38, and MEK, respectively, as activity readouts for these pathways (Fig. 3A). We performed independent experimental replicates on separate days (Fig. 3B) and then analyzed each experimental replicate using partial correlation as described above (Fig. 3C). We then merged the *P* values from the independent experimental replicates using a modified Fisher's method (*41, 42*). This analysis reproduced the negative partial correlation between the p38 and JNK pathways in the presence of p38 inhibition (partial correlation = −0.72, $q_{BH} < 10^{-8}$;

Fig. 3D). The increased significance observed here compared to above results from the increased statistical power by merging inferences across experimental replicates using Fisher's method. This analysis additionally revealed a significant negative partial correlation between the p38 and MEK pathways (partial correlation = −0.80, $q_{BH} < 10^{-10}$; Fig. 3D), demonstrating increased activation of both the MEK and JNK pathways by p38 inhibition. The positive partial correlation between p-CREB and p-Hsp27 (Fig. 3D) is the result of at least partial regulation of these nodes by p38 in SFs. This positive partial correlation for p38 inhibition coupled with the lack of a positive partial correlation between p-CREB and p-ERK for MEK inhibition (Fig. 3D) suggests that, although CREB is activated by both the p38 and MEK/ERK pathways (Fig. 1), CREB activity is primarily driven by the p38 pathway in SFs activated with IL-1α. The JNK inhibitor and the MEK inhibitor each enhanced p38 pathway activity; however, this effect was weaker than the converse effect of increased JNK and MEK pathway activity by p38 inhibition discussed above (Fig. 3, D and E). We did not detect cross-talk between JNK and MEK (Fig. 3D), despite such cross-talk being reported in other cell types (*43–45*). A traditional correlational analysis that does not control for the effect of IL-1α is dominated by the positive effect of IL-1α on MAPK signaling and fails to accurately characterize the presence or absence of multivariate inhibitor effects for the MEK, JNK, or p38 inhibitors (fig. S7). Overall, we conclude that the p38 pathway exhibits greater multipathway control in SFs than the other MAPK pathways MEK and JNK and that the inhibition of p38 results in significantly increased MEK and JNK signaling due to relief of this negative regulatory cross-talk.

Context dependence of pathway cross-talk
To further explore the relationship between stimulatory context and multipathway effects of p38 inhibition, we examined SF signaling responses on the background of the diverse signaling network states induced by IL-1α, TNFα, EGF, or IL-6. After 90 min of stimulation in
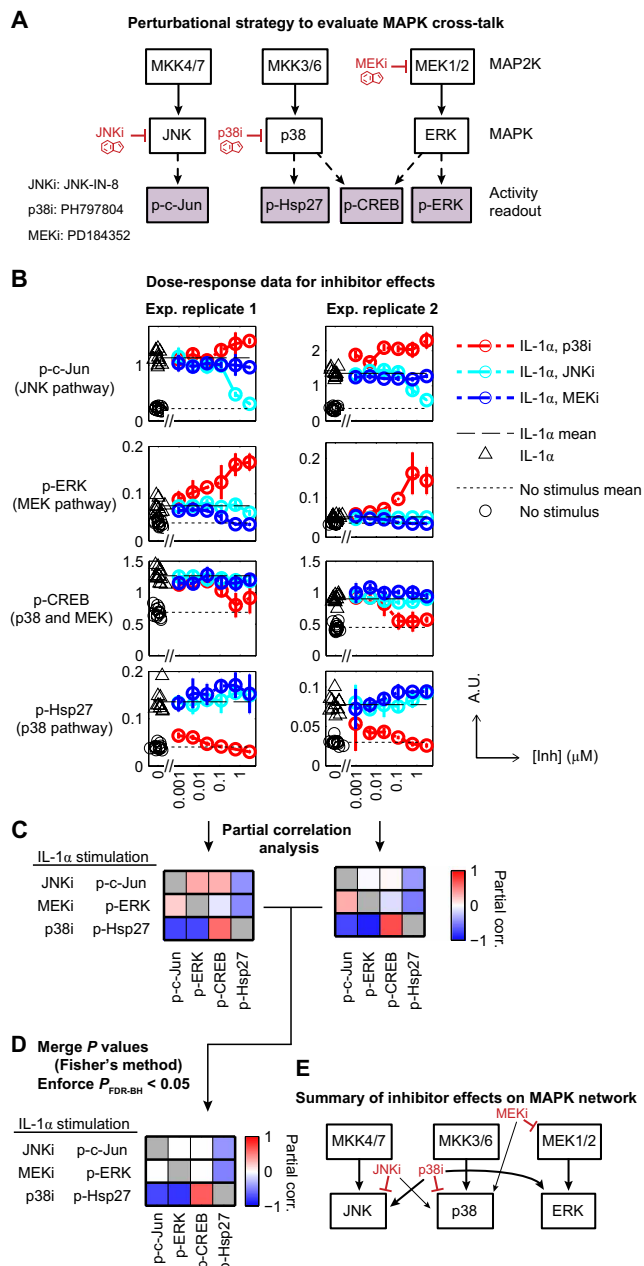
Fig. 3. Dominant role for p38 in cross-talk between the MAPK pathways p38, JNK, and MEK in SFs. (**A**) Perturbational strategy for evaluating mitogen-activated protein kinase (MAPK) cross-talk. (**B**) Dose-response data for specific p38, JNK, or MEK inhibitors after 90 min of stimulation with IL-1α (100 ng/ml). Titration was performed in biological quadruplicate on SF sample RA2159, and a full experimental replicate was repeated on a separate day (left versus right). A.U., arbitrary fluorescence units. (**C**) Experimental replicates were individually evaluated for partial correlation between inhibitor effect (rows) and MAPK signaling (columns) while controlling for the primary effect of IL-1α. Relevant proximal signaling measurements were used as a proxy to monitor canonical signaling downstream of a given inhibitor (for example, p-c-Jun was used as a surrogate for JNK pathway activity in the presence of the JNK inhibitor, p-ERK for MEK inhibition, and p-Hsp27 for p38 inhibition). "Self" partial correlation was excluded from the analysis (such as partial correlation between p-Hsp27 and p-Hsp27) and is shown in gray. (**D**) P values and partial correlations from the independent experiments were merged using a modified Fisher's method to allow for meta-analysis of two-sided P values (41, 42); partial correlations with q_{BH} (for the merged Fisher P values) ≥ 0.05 are set to 0. (**E**) Network summary of inferred inhibitor effects on MAPK signaling.

the presence or absence of the p38 inhibitor PH-797804, we measured the activation of 10 signaling proteins and transcription factors within the NF-κB, p38, MEK/ERK, PI3K/AKT, JNK, or JAK/STAT pathway using high-throughput microscopy (schematically depicted in fig. S8A). The experiment was repeated in the same SF donor sample on separate days, with one experimental replicate comprising titration of the p38 inhibitor in biological duplicate and the second experimental replicate comprising at least four biological replicates with the p38 inhibitor at a concentration above its 90% maximum inhibition (IC$_{90}$, 0.6 µM; fig. S8, B and C). We performed the partial correlation analysis as described above to evaluate the correlation between the effects of the p38 inhibitor on the p38 pathway (through p-Hsp27) and the alternative pathways when controlling for the primary effects of each individual stimulus. The two experimental replicates were analyzed separately, and P values were merged using the modified Fisher's method (41). We found that inhibiting the p38 pathway increased MEK, JNK, and NF-κB signaling within the context of IL-1α and TNFα stimulation [as evidenced by their negative partial correlation to p-Hsp27 for these stimuli (Fig. 4A)]. In the context of EGF stimulation, however, only JNK signaling was increased by p38 inhibition (Fig. 4A). To further examine cross-talk by p38, we evaluated additional p38 inhibitors, including four that were tested in phase II clinical trials for RA. The increased activation of IL-1α– and TNFα-induced NF-κB, JNK, and MEK pathways was consistent across all six p38 inhibitors (Fig. 4B). It was also consistent across TNFα and IL-1α concentrations ranging from 0.1 to 100 ng/ml (Fig. 4C), suggesting that such effects would be relevant in the face of variations of TNFα or IL-1α across patients or disease status. Together, this demonstrates that p38 inhibition elevates the activities of multiple alternative pathways, and these multipathway effects are most pronounced for inflammatory stimuli such as TNFα or IL-1α.

Notably, the enhancement of MEK signaling by p38 inhibition does not appear to propagate downstream to CREB (Fig. 4A). To explore this in more detail, we reanalyzed the data for MEK and p38 inhibition (from Fig. 3). We did not observe a significant pairwise correlation between MEK pathway activity (through p-ERK) and p-CREB (P = 0.66; Fig. 4D). However, controlling for the positive correlation between p-CREB and p38 pathway activity (through p-Hsp27; Fig. 4E) identified a significant positive relationship between MEK signaling and p-CREB (P = 2.2 × 10^{-6}; Fig. 4F). This suggests that the increased MEK/ERK signaling is propagated downstream to CREB, despite CREB activity in response to IL-1α stimulation being dominated by the p38 pathway. Moreover, these findings demonstrate the strength of combining broad perturbational experiments with multivariate analyses to identify network connections in the face of multiple confounding factors.

CREB as a key regulator of context-dependent cross-talk
To further evaluate the relationship between stimulatory context and multipathway effects of p38 inhibitors, as well as the relative absence of such effects for JNK and MEK inhibitors, we explored potential mechanisms of cross-talk by the p38, JNK, and MEK/ERK pathways. One method of cross-talk involves the regulation of phosphatases that act on neighboring pathways. The p38 and MEK/ERK pathways (through CREB) and JNK (through c-Jun) can each activate dual-specificity protein phosphatase 1 (DUSP1; also called MAP kinase phosphatase 1 or MKP-1), which provides negative feedback regulation to the p38 and JNK pathways (Fig. 5A) (25, 43, 46–48). A relatively specific inhibitor of DUSP1 (49) strongly elevated both p38 and JNK
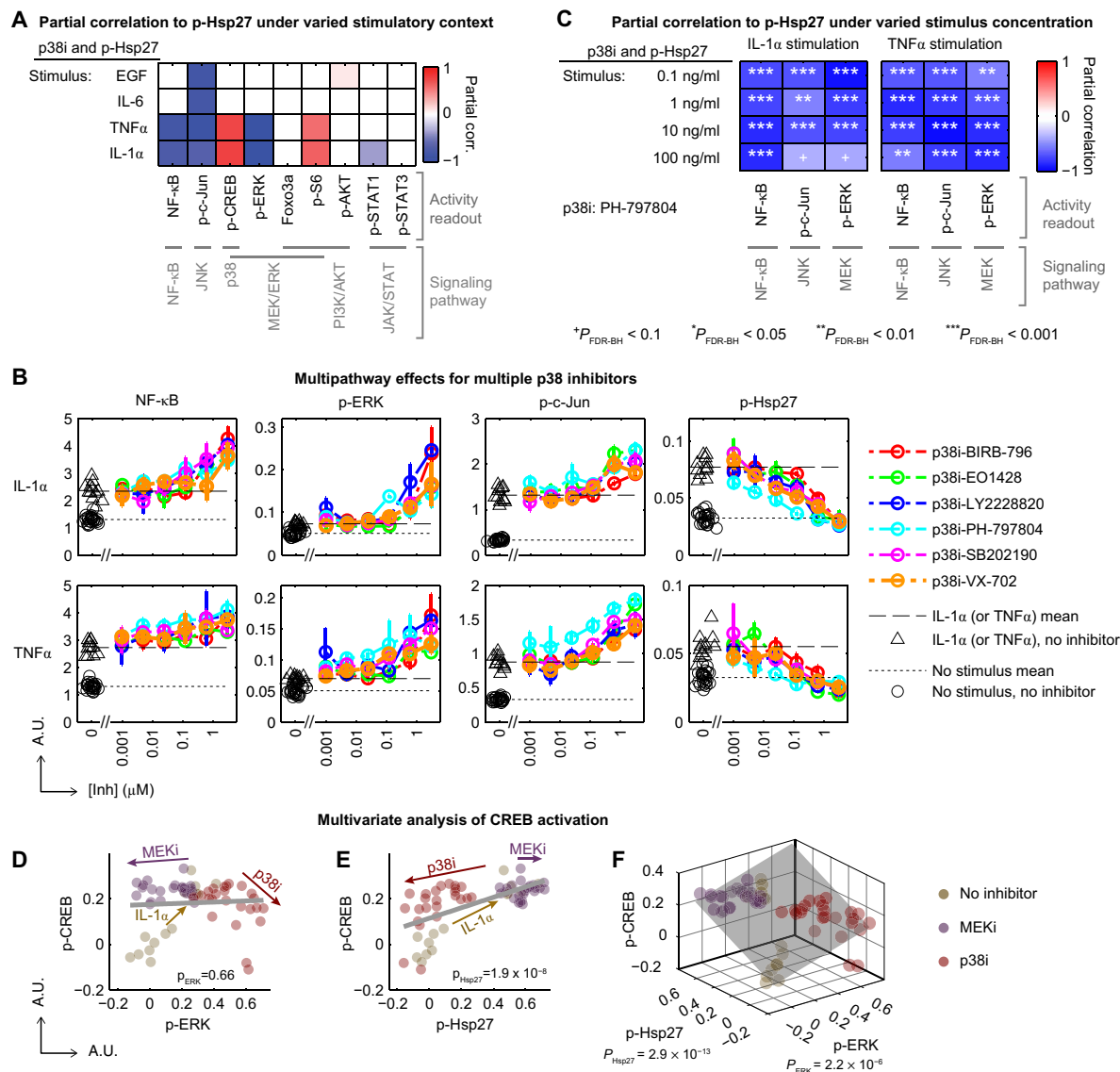
Fig. 4. Network-wide analysis of cross-talk by p38. (**A**) Partial correlation between p-Hsp27 (as a handle for p38 pathway activity; rows) and network proteins (columns) conferred by p38 inhibition. Signaling network activity was evaluated after 90 min of stimulation with EGF, IL-6, TNFα, or IL-1α (100 ng/ml each). Two experiments were performed on separate days on SF sample RA2159, with experiment 1 comprising titration of p38 inhibitor PH-797804 in biological duplicate and experiment 2 comprising four to six replicates of a single concentration of PH-797804 (0.6 μM). *P* values for the independent experimental replicates were merged using the modified Fisher's method (*41, 42*), and partial correlations with $q_{BH} \geq 0.05$ were set to 0. (**B**) Enhancement of nuclear factor κB (NF-κB), ERK, and c-Jun activation in SF sample RA2159 after 90 min of stimulation with IL-1α or TNFα (100 ng/ml each) by each of six p38 inhibitors, including four that were unsuccessfully evaluated in clinical trials for RA (BIRB-796, LY2228820, PH-797804, and VX-702). A.U., arbitrary fluorescence units. (**C**) Multipathway effects of PH-797804 across a concentration range (0.1 to 100 ng/ml) of IL-1α and TNFα. (**D** to **F**) Reanalysis of MEK- and p38-inhibitor (MEKi and p38i) data from Fig.3; univariate (D and E) and multivariate (F) analyses of correlations between p-ERK or p-Hsp27, and p-CREB.

pathway activities (Fig. 5B). In addition, SB747651A, which is a specific inhibitor of mitogen- and stress-activated protein kinases 1 and 2 (MSK1/2) and ribosomal protein S6 kinases 1 and 2 (RSK1/2), two structurally homologous upstream regulators of CREB (*50, 51*), increased p38 and JNK signaling in SFs (Fig. 5B). Combination of SB747651A with p38 inhibition, however, did not further augment IL-1α–induced JNK signaling relative to p38 inhibition alone (Fig. 5C). Together, these observations suggest that feedback regulation by DUSP1 at least partially mediates the p38-dependent pathway cross-talk that we observe in SFs. These data also underscore a role for CREB in feedback

regulation by p38 and are consistent with our observations above suggesting that p38 signaling plays a dominant role in CREB signaling in activated SFs.

The question remains, however, that if phosphatases that are regulated by JNK, p38, and ERK pathways mediate pathway cross-talk in SFs, why do p38 inhibitors show dominant multipathway effects in SFs, whereas JNK and MEK inhibitors are much more modest? We reasoned that context-dependent regulation of CREB signaling may play a role in the differential multipathway effects. To further explore this context dependence, we reanalyzed the SF network activation data
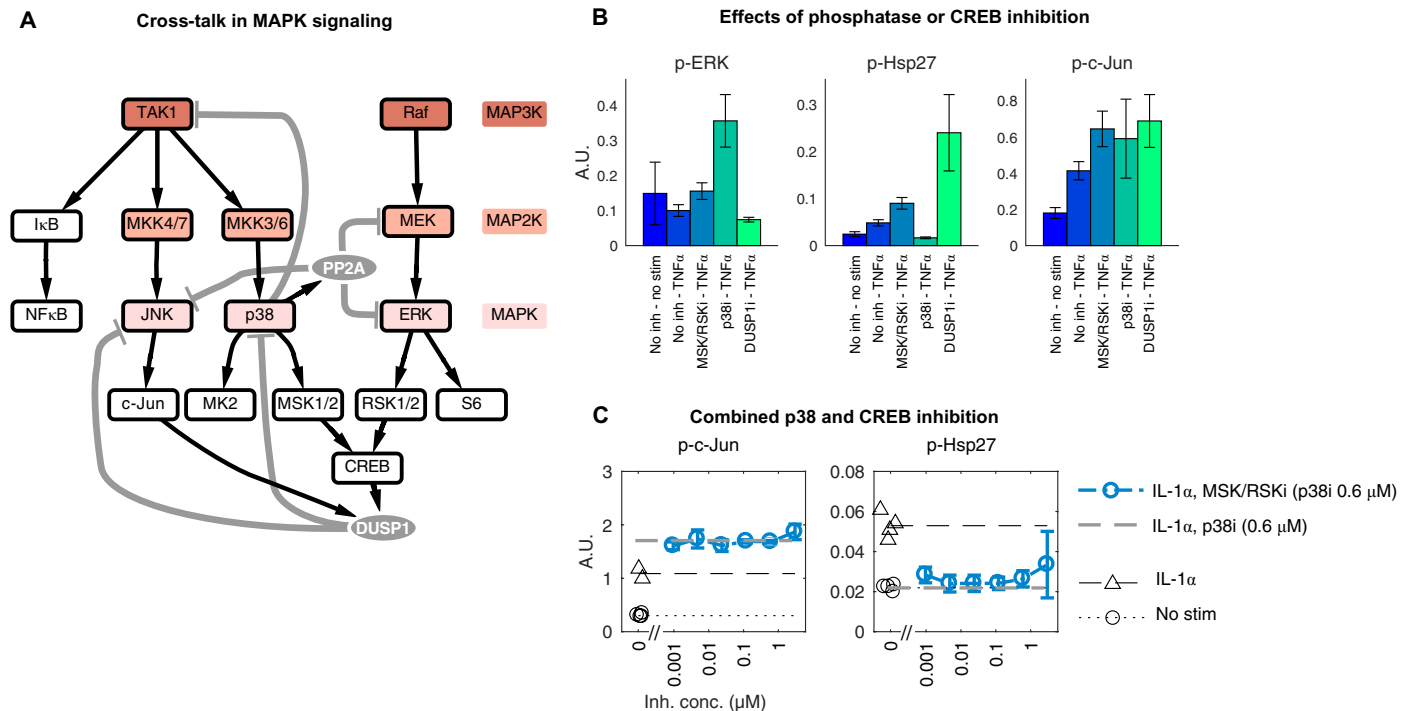
Fig. 5. Exploring MAPK regulation and cross-talk in SF. (**A**) Schematic depicting MAPK signaling and cross-talk. Phosphatases are shown as gray ovals, and negative regulatory feedback is shown as gray lines. (**B**) Effects of specific inhibitors of MSK/RSK (MSK/RSKi and SB747651A; 3 μM) or DUSP1 (DUSP1i and BCI; 3 μM) on MAPK signaling after 90 min of stimulation with TNFα (100 ng/ml). MSK1/2 and RSK1/2 are, respectively, p38- and MEK-dependent proximal upstream regulators of CREB. The p38 inhibitor PH-7978004 (p38i; 0.6 μM) was used for comparison. (**C**) Effects of the combination of MSK/RSKi and p38i on c-Jun and Hsp27 phosphorylation after 90 min of stimulation. A.U., arbitrary fluorescence units.

(from Fig. 1) by averaging the MLR β coefficients across time and RA SF sample and plotting as a node-edge graph in which the width of the edge is proportional to the strength of the averaged β coefficients (Fig. 6A). Although many of the same pathways are activated by the inflammatory stimuli IL-1α and TNFα, and the mitogenic stimulus EGF, these stimuli differ strongly in their magnitude of activation: IL-1α and TNFα more strongly activate the NF-κB, JNK, and p38 pathways, whereas EGF more strongly activates the MEK/ERK pathway (Fig. 6A). We further reanalyzed the kinetics of p38 and MEK activation by TNFα, IL-1α, and EGF and found that although these stimuli induced different dynamics for MEK/ERK and p38 signaling, they nevertheless converged to consistent signaling at the level of CREB (Fig. 6B). We conclude that CREB acts as an integrator of p38 and MEK/ERK pathway activities and its activation is dominated by p38 signaling in response to TNFα and IL-1α, but by MEK/ERK signaling in response to EGF.

To explore a role for CREB in context-dependent cross-talk in SFs, we evaluated the multipathway effects of MEK and p38 inhibitors under mitogenic and inflammatory contexts. Notably, whereas MEK inhibition minimally affected p38 pathway activity within the context of IL-1α stimulation (Fig. 3), it strongly increased EGF-induced p38 activity (as assayed by p-Hsp27) (Fig. 6C). These relationships are reversed from that of the p38 pathway: p38 inhibition minimally affected EGF-induced MEK/ERK pathway activity (Fig. 6B), in contrast to its strong enhancement of IL-1α– or TNFα-induced MEK/ERK activity (Fig. 4, A to C). The more limited multipathway effects of p38 inhibition for EGF stimulation as compared to IL-1α or TNFα stimulation were consistent across four normal and four RA SF samples (Fig. 6D and fig. S9) and across dermal fibroblast and mammary epithelial cell lines

(Fig. 6E), suggesting that the context dependence characterized in this study is a general feature of p38 signaling. Overall, these data reveal a critical role for CREB signaling in context-dependent multipathway cross-talk by the MEK/ERK or p38 pathways and demonstrate how stimulatory environment influences which pathways dominate cross-talk even within a fixed signaling network topology (Fig. 6F). This in turn results in marked differences for the effects of drugs targeting MEK or p38 depending on whether the context is inflammatory or mitogenic.

Decoupling pathway cross-talk and pathway inhibition

To assess whether inhibiting additional pathways could decouple the multipathway effects of p38 inhibition, we evaluated combinations of JNK or MEK inhibitors with p38 inhibition. Titration of the JNK inhibitor JNK-IN-8 in the presence of IL-1α and the p38 inhibitor PH-797804 blocked the enhanced activation of the JNK pathway in a dose-dependent manner as expected, but did not mitigate that of NF-κB or MEK signaling by the p38 inhibitor (fig. S10A). Similarly, titration of the MEK inhibitor PD325901 in the presence of IL-1α and PH-797804 specifically blocked cross-talk to the MEK pathway. This combination did, however, result in further enhancement of NF-κB nuclear translocation beyond that of p38 inhibition alone (fig. S10B). Notably, MEK inhibition in the absence of the p38 inhibitor did not affect NF-κB nuclear translocation (fig. S10C), suggesting coordinate down-regulation of NF-κB signaling by p38 and MEK signaling.

We further evaluated whether inhibitors against nodes upstream or downstream of p38 could also decouple the desirable inhibition from the pathway cross-talk. Transforming growth factor β–activated kinase 1 (TAK1; also known as MAP3K7) lies upstream of p38, JNK,
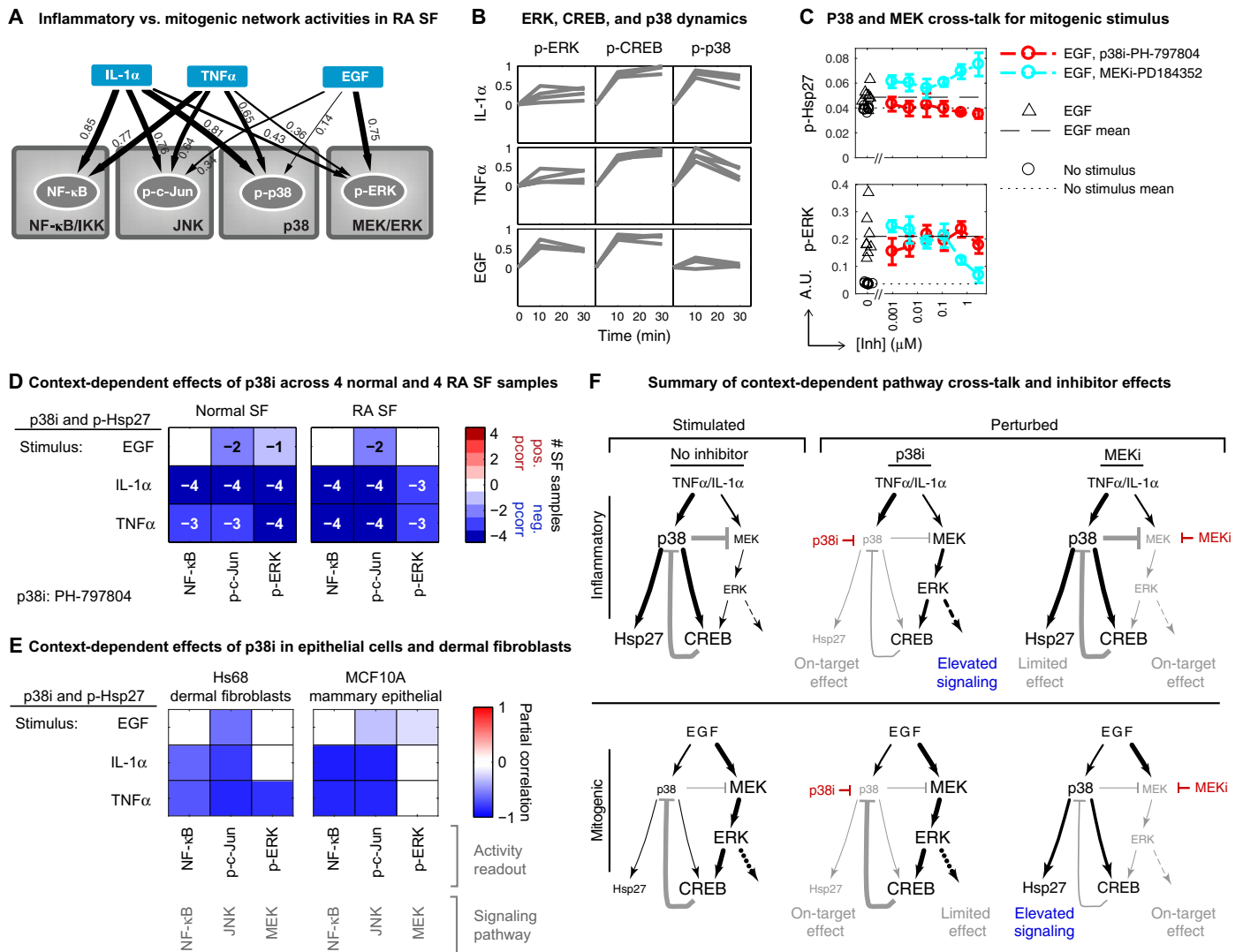
Fig. 6. Inflammatory versus mitogenic stimulatory context dependence of p38 and MEK inhibitors. (**A**) Node-edge graph of selected β coefficients from Fig.1 (and fig. S5) showing relative magnitudes of pathway activation by TNFα, IL-1α, or EGF. Edge thickness is proportional to strength of MLR β coefficients that were averaged across time and RA SF sample for each node. (**B**) β coefficients of p-ERK, p-CREB, and p-p38 for RA SF samples plotted as a time course. Coefficients were scaled to a maximum of 1 for each node across all time points, SF samples, stimuli, and experimental replicates. (**C**) Effects of p38 or MEK inhibition on EGF-induced signaling in SF sample RA2159 [after 90 min of incubation with EGF (100 ng/ml)]. (**D**) Partial correlation to p-Hsp27 across four normal or four RA SF samples; showing consistent context-dependent multipathway effects for p38 inhibition across SF samples. Nuclear translocation (for NF-κB) or phosphorylation was measured after 90 min of stimulation with EGF, IL-1α, or TNFα (100 ng/ml each). (**E**) Partial correlation to p-Hsp27 for EGF, IL-1α, or TNFα stimulation (100 ng/ml each for 90 min) in Hs68 dermal fibroblasts (left) or MCF10A mammary epithelial cells (right), showing similar context dependence to that observed in SF samples. Hs68 or MCF10A cells were treated in biological quadruplicate, and the full experiment was repeated across separate days. P values for the independent experimental replicates were merged using the modified Fisher's method (41, 42), and partial correlations with $q_{BH} \geq 0.05$ were set to 0. (**F**) Schematic summarizing p38 and MEK inhibitor effects in inflammatory versus mitogenic contexts.

and NF-κB signaling (Fig. 5A) and regulates much of the inflammatory cytokine secretion by activated SF in RA (*12*). The TAK1 inhibitor (5z)-7-oxozeaenol (5ZO) inhibited both the primary activation of NF-κB, JNK, p38, and MEK/ERK signaling induced by TNFα and IL-1α (fig. S11A) and blocked the increased signaling conferred by p38 inhibition (fig. S11B). Known polypharmacology of 5ZO toward MEK1/2 (International Centre for Kinase Profiling, www.kinase-screen. mrc.ac.uk/kinase-inhibitors) likely contributes to the inhibition of ERK activation that we observe here. MAPKAPK2 (or MK2) lies downstream of p38 and promotes inflammatory cytokine production (*23*). In contrast to direct p38 inhibition, MK2 inhibition did not ex-

hibit multipathway effects (fig. S11C). We conclude that combinations of MAPK inhibitors or inhibition of nodes upstream or downstream of p38 can decouple multipathway cross-talk to result in more effective suppression of inflammatory signaling in SFs.

Activation of SFs by RA synovial fluids
On the basis of the understanding of the SF signaling network developed above, we examined pathways activated in SFs by the disease-relevant context of RA synovial fluids. SFs from one RA donor were exposed to serially diluted RA synovial fluids, and signaling activation was measured using high-throughput immunofluorescence microscopy.

Because of limited quantities of RA synovial fluids, we pooled equal volumes of fluids from two RA patients and diluted them in basal SF medium (pooled RA Fluids_CD; information on synovial fluids is in table S4). Synovial fluid naturally functions as a joint lubricant and is present in only very small amounts in healthy patients; synovial fluids from healthy individuals were, thus, not available for comparison due to challenges in collecting such material (*52*). The pooled RA synovial fluids significantly activated the JNK, MEK, and p38 pathways (through p-c-Jun, p-ERK, and p-Hsp27, respectively; Student's *t* test, $P < 10^{-9}$) and reached similar levels of activation as saturating doses of TNFα (Fig. 7A). Up to
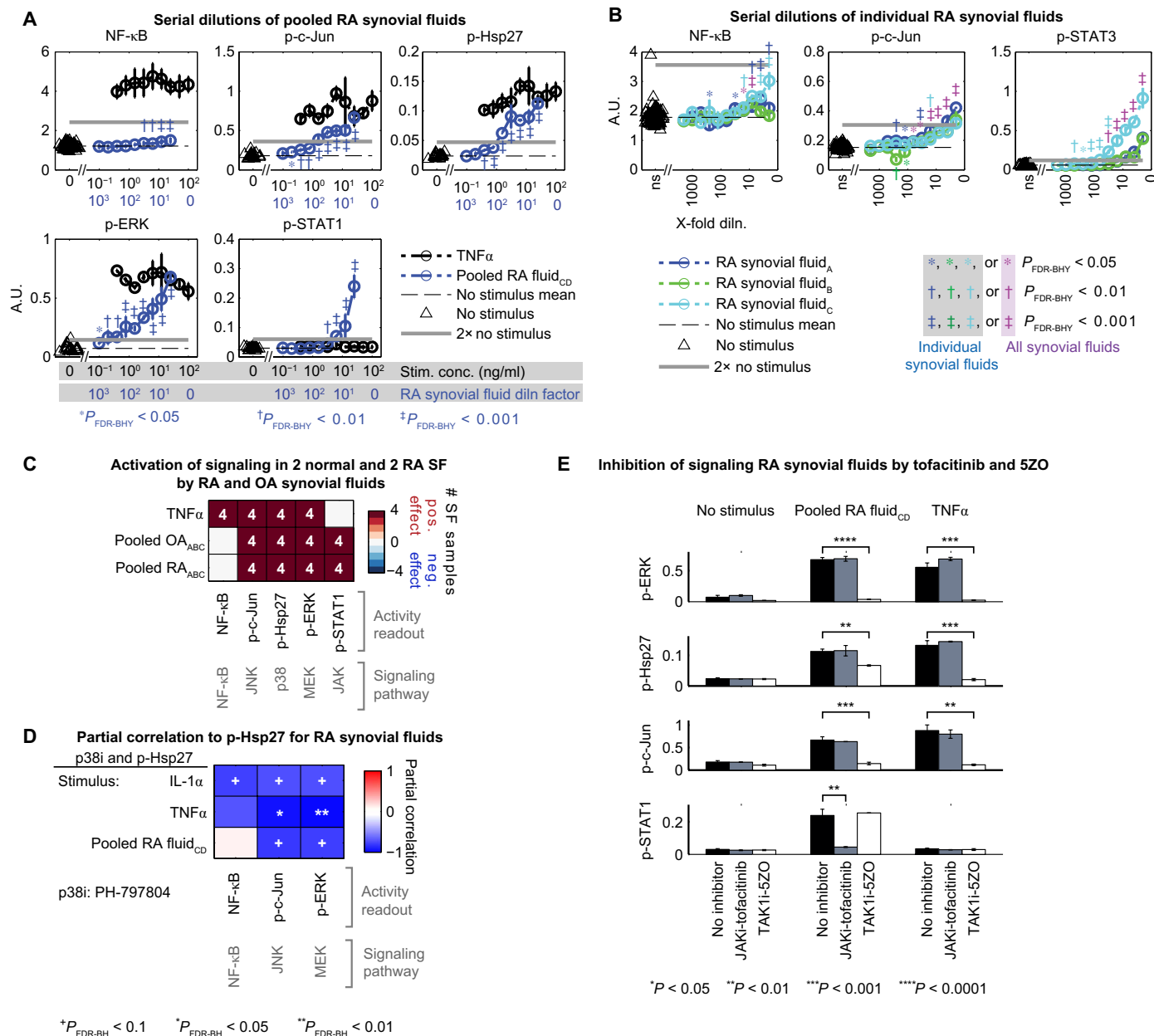
Fig. 7. Activation of SF signaling by RA synovial fluids. (**A**) Activation of signaling in SFs by serial twofold dilution of pooled RA synovial fluids into basal SF media (1:4 to 1:1024 dilution series of an equal volume mixture of RA fluid samples C and D); serial twofold dilution of TNFα (0.4 to 100 ng/ml) was used as a positive control for NF-κB (nuclear translocation), p-c-Jun, p-Hsp27, and p-ERK. Data are means ± SD. (**B**) Serial twofold dilution of individual RA synovial fluid samples A, B, and C (1:2 to 1:2048 dilution series). (**C**) Consistency of signaling activation across two normal and two RA SF samples (as determined by MLR analyses) by 1:4 dilution of pooled RA synovial fluids (equal volumes of RA fluid samples A, B, and C) or pooled osteoarthritis (OA) synovial fluids (equal volumes of OA fluid samples A, B, and C). (**D**) Partial correlation analysis for p38 inhibition augmenting signaling induced by pooled RA synovial fluids. (**E**) Effects of tofacitinib (1.5 μM) or 5ZO (1.0 μM) on signaling induced by 1:4 dilution of pooled RA synovial fluids (30 min of stimulation with equal volume mixture of RA synovial fluid samples C and D). TNFα (100 ng/ml) was used as a positive control. Data are means ± SD. Signals were measured in biological duplicate after 30 min (A to C and E) or 90 min (D) of stimulation in SF sample RA2159 (A, B, D, and E) or samples N2586, N2759, RA2159, and RA2708 (C). Significance was determined by an unpaired two-sample Student's *t* test (synovial fluid dilutions versus unstimulated signal; A and B); false discovery rate was controlled using the Benjamini-Hochberg-Yekutieli method for positive dependence (q_{BHY}) (*69*).

64-fold dilution of the pooled RA synovial fluids continued stimulating activation of these pathways to at least twofold above unstimulated levels (Fig. 7A). The RA synovial fluids also significantly activated p-STAT1 ($P < 10^{-14}$), with up to 16-fold dilution of the pooled RA fluids, resulting in p-STAT1 activation to at least twofold above the assay background (Fig. 7A). We detected statistically significant nuclear translocation of NF-κB ($P < 10^{-8}$), but the effect size was smaller than activation of MAPK or JAK/STAT signaling (Fig. 7A). Individual evaluation of RA synovial fluids from three separate patients resulted in nuclear translocation of NF-κB (up to 1.5-fold assay background) in one of the RA synovial fluid samples and increased activation of p-STAT3 by the same sample, suggesting that RA synovial fluids from different donors can variably activate SF signaling (Fig. 7B). Moreover, this demonstrates that RA synovial fluids can activate both proinflammatory (STAT1; Fig. 7A) and antiapoptotic, pro-proliferative (STAT3; Fig. 7B) branches of the JAK/STAT pathway in SFs (53), which would support both the proinflammatory and hyperplasia phenotypes of activated SFs in RA. The pathways activated by RA synovial fluids were consistent across SFs from two normal and two RA donors (Fig. 7C and fig. S12A). Notably, pooled OA synovial fluids exhibited similar activity to RA synovial fluids on both normal and RA SFs (Fig. 7C and fig. S12A). We conclude that inflammatory factors in RA and OA synovial fluids strongly activate intracellular kinase signaling in SFs, and this signaling response is consistent across SFs from normal and RA donors.

Because synovial fluids activate many of the pathways that are regulated by TAK1 in activated SFs or increased by p38 inhibitors in inflammatory contexts, we investigated the effects of p38 or TAK1 inhibition on the activation of SFs by RA synovial fluid. Because of limited quantities of RA synovial fluids, we examined a single concentration of the p38 inhibitor (PH-797804 at 0.6 μM) in biological duplicate (fig. S12B). Inhibition of p38 increased the activity of both MEK and JNK pathways induced by the RA synovial fluids, consistent with our previous observations for stimulation with IL-1α or TNFα (partial correlation = −0.77 and −0.79, $q_{BH} < 0.1$; Fig. 7D). We then compared the effects of the TAK1 inhibitor 5ZO with the FDA-approved JAK inhibitor tofacitinib. Whereas tofacitinib inhibited only JAK/STAT signaling, 5ZO significantly inhibited activation of the JNK, p38, and MEK/ERK pathways induced by RA synovial fluids and not the JAK/STAT pathway (Fig. 7E). Together, this demonstrates that p38 inhibition elicits compensatory signaling responses within the complex environment of RA synovial fluids. By comparison, 5ZO is capable of normalizing SF activation in a manner that is complementary to existing treatment options for RA.

DISCUSSION

Here, we used a systematic approach to analyze the multivariate effects of kinase inhibitors on inflammatory signaling responses. The effects of the inhibitors were complex and challenged traditional approaches for evaluating intracellular signaling. We therefore applied an analytical framework that controlled for multiple confounding factors while identifying statistically significant associations within the data. We found that p38 functioned as a uniquely central node that regulated the activity of multiple other pathways specifically in inflammatory, but not mitogenic, contexts, and its inhibition strongly increased NF-κB, JNK, and MEK/ERK activity. Such an effect is clinically undesirable given the connections of these pathways to inflammation and RA progression (7, 54, 55) and likely played a role limiting the clinical benefit of p38 inhibitors for RA.

A characteristic feature of RA is a self-sustaining inflammatory microenvironment in affected joints. Our findings suggest that SFs function in a positive feedback loop to help sustain this microenvironment. RA synovial fluids provoked a strong inflammatory signaling response in ex vivo cultures of SFs and induced the activation of the p38, JNK, and MEK pathways to similar levels as saturating amounts of TNFα. Whereas RA SFs display a uniquely aggressive phenotype (7, 9), we observed similar activation of both normal and RA SFs by RA synovial fluids. These findings suggest that soluble factors from the RA microenvironment prime the resident SFs toward the aggressive, activated phenotype observed in RA. We have previously reported that cytokines secreted by ex vivo cultures of activated SFs are enriched in the synovial fluids of RA patients (12). Activated SFs are also capable of presenting arthritogenic peptides to T cells, further promoting RA pathogenesis (56). Together, these observations support a complex relationship between SFs and their environment in RA, in which SFs are directly activated by the inflamed RA microenvironment and activated SFs further perpetuate this inflammation and autoimmunity.

Intracellular signaling pathways are highly interconnected, and in this study, we found a critical role for stimulatory context in determining which signaling pathway dominates negative regulatory cross-talk. Such a context dependence resulted in marked differences in drug effects depending on stimulatory context and has strong implications for understanding how successful versus unsuccessful therapeutic interventions may be biologically conditioned. For example, we found contrasting effects of drugs targeting p38 or MEK depending on whether the context was primarily inflammatory or mitogenic: p38 inhibitors exhibited greater multipathway effects in proinflammatory environments, whereas multipathway effects of MEK inhibition were more prominent for mitogenic than inflammatory contexts.

CREB emerged as a key nexus for these context-dependent inhibitor effects. It is activated by both the MEK and p38 pathways, and upon activation, it regulates expression of phosphatases that down-regulate MAPK activity (47, 48). CREB thus functions in part within a negative regulatory feedback loop for MAPK signaling. We found that stimulatory context strongly influenced the regulation of CREB by the MEK or p38 pathways: For the inflammatory stimuli TNFα and IL-1α, CREB activity is dominated by the p38 pathway, whereas for the mitogenic stimulus EGF, CREB activity is dominated by the MEK/ERK pathway. We reason that feedback via a MEK/CREB axis is suppressed in inflammatory contexts due to the dominance of p38 on CREB activity. For mitogenic contexts, the converse is true: The dominance of MEK signaling on CREB activity suppresses potential negative regulatory feedback from a p38/CREB axis. The p38 pathway can provide additional negative regulatory feedback through its activation of protein phosphatase 2A (PP2A), which negatively regulates JNK and MEK/ERK activity (57, 58), and through negative regulatory feedback to TAK1, an upstream regulator of p38, JNK, and NF-κB signaling (Fig. 5A) (59, 60). For stimulatory contexts that strongly activate p38, these additional mechanisms of cross-talk would further strengthen the role of p38 in down-regulating activated intracellular signaling.

Although p38 inhibition is no longer under clinical investigation for RA, it has generated interest for a range of disorders involving dysregulated inflammation such as multiple sclerosis (61), chronic obstructive pulmonary disorder (62), atherosclerosis (63, 64), diabetic cardiomyopathy (65), and neuropathic pain (66, 67). Our findings argue for careful analysis of the effects of p38 inhibitors on multiple potential compensatory pathways and on the background of multiple

disease-relevant contexts to understand the full effects of drugs targeting p38 in inflammation-related disorders. We found that cross-talk by p38 could be decoupled through combinations of inhibitors or by targeting nodes upstream or downstream of p38, such as TAK1 or MK2. This suggests that alternative therapeutic strategies can maintain at least part of the benefits of direct p38 inhibition while limiting the undesirable effects of relieving negative regulatory cross-talk by p38. More broadly, our work suggests that a more systematic analysis of potential multipathway effects of drug candidates should be included as part of a clinical development program. Such experimentation and analysis can help clarify the risks of developing drugs targeting nodes believed to be involved in multipathway cross-talk.

MATERIALS AND METHODS
Antibodies and reagents
TNFα (cat. no. 300-01A), IL-1α (cat. no. 200-01A), IL-6 (cat. no. 200-06), and EGF (cat. no. AF-100-15) were purchased from PeproTech. Chemical inhibitors from the following sources were dissolved in dimethyl sulfoxide (DMSO) to 10 mM stock concentrations: TAK1 inhibitor 5ZO (cat. no. 3604), p38 inhibitor EO 1428 (cat. no. 2908), and MSK/RSK inhibitor SB747651A (cat. no. 4630) were purchased from Tocris Bioscience; p38 inhibitors PH-797804 (cat. no. S2726), SB202190 (cat. no. S1077), VX-702 (cat. no. S6005), BIRB-796 (cat. no. S1574), and LY2228820 (cat. no. S1494), MEK inhibitor PD184352 (also referred to as CI-1040; cat. no. S1020), and JAK inhibitor tofacitinib (also referred to as CP-690550; cat. no. S2789) were purchased from Selleck Chemicals; DUSP1/6 inhibitor BCI [(E)-2-benzylidene-3-(cyclohexylamino)-2,3-dihydro-1H-inden-1-one] was purchased from Axon Medchem (cat. no. 2178); MK2 inhibitor III (cat. no. 475864) and inhibitor IV (cat. no. 475964) were purchased from EMD Millipore; JNK inhibitor JNK-IN-8 was provided by the Nathanael Gray Laboratory, Dana-Farber Cancer Institute (DFCI). Antibodies to p-p44/42 MAPK (ERK1/2) Thr^{202}/Tyr^{204} (cat. no. 4370), p-Hsp27 Ser^{82} (cat. no. 9709), p-c-Jun Ser^{73} (cat. no. 3270), p-STAT1 Tyr^{701} (cat. no. 9167), p-STAT3 Tyr^{705} (cat. no. 9145), p-S6 Ser$^{235/236}$ (cat. no. 4858), p-CREB Ser^{133} (cat. no. 9198), p-AKT Ser^{473} (cat. no. 4060), p-MK2 Thr^{334} (cat. no. 3007), p-JNK Thr^{183}/Tyr^{185} (cat. no. 9251), p-p38 Thr^{180}/Tyr^{182} (cat. no. 4511), FoxO3a (cat. no. 2497), and NF-κB p65 (cat. no. 8242) were purchased from Cell Signaling Technology. Antibody to NF-κB p65 (cat. no. sc-8008) was purchased from Santa Cruz Biotechnology. Fluorescently labeled secondary antibodies donkey anti-mouse immunoglobulin G (IgG) polyclonal antibody (pAb) Alexa 488 conjugate (cat. no. A21202) and donkey anti-rabbit IgG pAb Alexa 647 conjugate (cat. no. A31573) were purchased from Thermo Fisher Scientific. RA synovial fluids were purchased from Analytical Biological Services Inc. and provided by J. Swantek at Boehringer Ingelheim Inc. (table S4).

Tissue culture
Normal primary human SFs [human fibroblast-like synovioctyes (HFLS), cat. no. 408-05a] and RA SFs (HFLS-RA, cat. no. 408RA-05a) were purchased from Cell Applications Inc. (table S2). The nomenclature used for SF samples denotes lot number (for example, N2586 is Cell Applications HFLS lot no. 2586, RA2159 is Cell Applications HFLS-RA lot no. 2159, etc.). Cells were cultured according to the supplier's recommendations using Synoviocyte Growth Medium (Cell Applications Inc., cat. no. 415-500), and Synoviocyte Basal Medium (Cell Applications Inc., cat. no. 414-500) was used for serum starvation before experimental treatments. Cells were provided at passage 2, and all experiments were conducted at passages 3 to 6, in line with published recommendations (68).

Signaling response seeding and treatments
Signaling responses of cultured SF were examined as previously described (12). Briefly, SFs were seeded (600 cells per well) into 384-well plates; after ~24 hours of incubation in full growth medium, cells were starved in basal medium overnight (~16 hours) followed by a refresh of basal medium approximately 4 hours before exposure to stimulatory factors. For experiments involving inhibitors, cells were pretreated with inhibitor or DMSO control for ~2.5 hours before stimulation with TNFα, IL-1α, IL-6, or EGF (100 ng/ml each) (diluted into basal SF medium containing 0.1% bovine serum albumin) at a final volume of 50 µl per well; DMSO was maintained at a constant concentration for all experimental treatments (for example, for experiments with a maximum inhibitor concentration of 3 µM, DMSO was maintained at a 1:3333 dilution for all treatments in the experiment, which corresponds to the amount of DMSO in 3 µM inhibitor diluted from a 10 mM stock concentration). To support reproducibility, all inhibitor and stimulus treatments were performed using automated liquid handling instruments (Biomek FX by Beckman Coulter or ID STARlet by Hamilton) at the Harvard Medical School Longwood Screening Facility.

Immunofluorescence microscopy and analysis
Measurement of signaling intensity by immunofluorescence microscopy was conducted as previously described (12). Briefly, cells were fixed in 2% paraformaldehyde for 10 min, washed three times for 5 min in 1× phosphate-buffered saline with 0.1% Tween 20 (PBST), permeabilized with 100% methanol for 10 min, washed three times with PBST, and blocked with Odyssey Blocking Buffer (OBB; LI-COR) for 1 hour. Cells were stained overnight at 4°C with 25 µl of primary antibodies diluted in OBB (see table S1 for dilution ratios for each antibody). Cells were washed three times with PBST and stained with 25 µl of appropriate secondary antibodies diluted at 1:2000 in OBB and incubated 1 hour. Cells were washed once in PBST and once in PBS and incubated with Hoechst 33342 (0.25 µg/ml; Invitrogen, cat. no. H3570) and Whole Cell Stain Green or Blue (1:1000 dilution; Thermo Fisher, cat. nos. 8403202 and 8403502) in PBS for 30 min. Cells were washed twice in PBS and imaged using a 10× objective on an Operetta high-throughput microscope using Harmony software (PerkinElmer Inc.).

Data were extracted from images using Columbus software (PerkinElmer Inc.). Briefly, Hoechst 33342 and Whole Cell Stain Green (or Whole Cell Stain Blue) signals were used to segment the nuclear and cellular boundaries. These segmented boundaries were then used to define nuclear, cytoplasmic, and whole-cell "regions" that were more narrowly defined than the segmented boundaries to accommodate potential errors by automated segmentation (see fig. S1). We defined "ring regions" for each cell to control for fluctuations in the local background (for example, because of dust, bubbles, or nonflat illumination). The ring regions comprised the 5 to 12 pixels beyond the cellular segmented boundary that was devoid of neighboring segmented cells. Cell-specific local background intensity was quantified from the individual ring regions and used to normalize signals for nuclear, cytoplasmic, and whole-cell regions. To quantify NF-κB nuclear translocation, nuclear/cytoplasmic ratios were calculated for each cell. For other signals, single-cell intensities were extracted for the appropriate cellular region; for example, nuclear intensity was used for phosphorylated transcription factors such as p-c-Jun, p-STAT1, and p-STAT3, whereas whole-cell or cytoplasmic intensity was used for p-ERK1/2

and p-HSP27 (see table S1 for cellular regions for each measured signaling protein). Median values of single-cell distributions within an individual well were used for all subsequent analyses.

MLR of signaling network responses

An MLR framework of the form $y = X\beta + \varepsilon$ was used to infer connections between stimuli and signaling network proteins from perturbational data. The predictor matrix X encodes an experimental design matrix, with the columns denoting the presence (1) or absence (0) of a given stimulus and the rows denoting individual experimental conditions; unstimulated background was denoted as a column of 1s. The response matrix y comprises the measured signal intensities for the experimental conditions (rows) across each measured signaling protein or transcription factor (columns). β is a vector of regression coefficients relating the effects of the stimuli in X to the signals in y; and ε is a vector of model residuals. We used MLR to solve for the β coefficients using the Matlab regstats.m function. This approach was used for each donor sample, time point, and independent experimental replicate.

For a multivariate analysis of inhibitor effects, MLR β coefficients for each signaling network protein were scaled to a maximum of 1 for the maximum value observed across all stimulatory contexts, SF samples, experimental replicates, and time points. Scaled MLR coefficients were then compiled across all conditions (4 stimuli × 8 SF samples × 2 experimental replicates = 64 rows) and all signaling network proteins and times points (13 signaling proteins × 2 time points = 26 columns). The matrix of compiled MLR coefficients was mean-centered (column-wise) and then analyzed by PCA using the Matlab pca.m function.

Consistency of network activation across donors

To evaluate consistency of network activation across SF samples, we first merged the P values of the independent experimental replicates for a given time point and SF sample using a modified Fisher's method, which allows the use of two-sided P values (41, 42), and controlled for the FDR of the resulting merged P values using the Benjamini-Hochberg method (34). To account for dynamics of a given signal, which may be active at one time point, but not another, a connection between a given stimulus and a given signal was taken to be present if the FDR-corrected, merged P value was less than 0.01 at either time point (10 or 30 min after stimulation; see fig. S3). The strength of a connection was determined by merging MLR coefficients across experimental replicates and time. The consistency of connections was summed across the eight SF samples (from four normal and four RA).

Partial correlation

Partial correlation is useful for evaluating correlations between pairs of variables while controlling for the variance explained by a third variable. We used this approach to evaluate correlations induced by specific pathway inhibitors using data from multiperturbational experiments. Briefly, data were $\log_{10}$-transformed and basal signal (no stimulus and no inhibitor) was set to 0 for each signaling network protein, and then the variance explained by stimuli was controlled using the MLR framework described above. The residuals of this model (ε) contain information about the effect of inhibitors. Data for a downstream signaling node were used as a handle for monitoring the effect of inhibitor titrations on pathway activities: p-Hsp27 was used as a handle for p38 pathway activity with the p38 inhibitor; p-c-Jun was used for JNK pathway activity with the JNK inhibitor; and p-ERK was

used for MERK/ERK pathway activity with the MEK inhibitor. The residuals for each stimulus and inhibitor context were partitioned along with a randomly selected subset of the control replicates (basal levels and stimulus in the absence of inhibitor) to avoid repeated use of control samples. Finally, for each stimulus and inhibitor context, we calculated the correlation between residuals of the respective proximal pathway target and other signaling network proteins using the Matlab corr.m function. These correlations between residuals are the reported partial correlations. P values for independent experimental replicates conducted on separate days were merged using a modified Fisher's method (41, 42), and FDR from multiple hypothesis testing was controlled using the Benjamini-Hochberg method (34).

Statistical analysis of serial dilutions and tofacitinib and 5ZO effects

Data were $\log_{10}$-transformed to stabilize variance. Significance of stimulated response data in comparison to the unstimulated signal was evaluated using an unpaired two-sample Student's t test with equal variance using the Matlab ttest2.m function. FDR for the RA synovial fluid serial dilutions was controlled using the Benjamini-Hochberg-Yekutieli method for positive dependence (69). Significance of tofacitinib or 5ZO inhibitor effects in comparison to the uninhibited stimulated signal was evaluated using an unpaired two-sample Student's t test with equal variance using the Matlab ttest2.m function.

REFERENCES AND NOTES
1. D. L. Scott, F. Wolfe, T. W. J. Huizinga, Rheumatoid arthritis. *Lancet* **376**, 1094–1108 (2010).
2. I. B. McInnes, G. Schett, The pathogenesis of rheumatoid arthritis. *N. Engl. J. Med.* **365**, 2205–2219 (2011).
3. S. Dadoun, N. Zeboulon-Ktorza, C. Combescure, M. Elhai, S. Rozenberg, L. Gossec, B. Fautrel, Mortality in rheumatoid arthritis over the last fifty years: Systematic review and meta-analysis. *Joint Bone Spine* **80**, 29–33 (2013).
4. G. S. Firestein, Evolving concepts of rheumatoid arthritis. *Nature* **423**, 356–361 (2003).
5. D. A. Fox, The role of T cells in the immunopathogenesis of rheumatoid arthritis. New perspectives. *Arthritis Rheum.* **40**, 598–609 (1997).
6. E. Neumann, S. Lefèvre, B. Zimmermann, S. Gay, U. Müller-Ladner, Rheumatoid arthritis progression mediated by activated synovial fibroblasts. *Trends Mol. Med.* **16**, 458–468 (2010).
7. N. Bottini, G. S. Firestein, Duality of fibroblast-like synoviocytes in RA: Passive responders and imprinted aggressors. *Nat. Rev. Rheumatol.* **9**, 24–33 (2013).
8. H. P. Kiener, G. F. M. Watts, Y. Cui, J. Wright, T. S. Thornhill, M. Sköld, S. M. Behar, B. Niederreiter, J. Lu, M. Cernadas, A. J. Coyle, G. P. Sims, J. Smolen, M. L. Warman,

M. B. Brenner, D. M. Lee, Synovial fibroblasts self-direct multicellular lining architecture and synthetic function in three-dimensional organ culture. *Arthritis Rheum.* **62**, 742–752 (2010).

9. A. Filer, The fibroblast as a therapeutic target in rheumatoid arthritis. *Curr. Opin. Pharmacol.* **13**, 413–419 (2013).

10. B. Bartok, G. S. Firestein, Fibroblast-like synoviocytes: Key effector cells in rheumatoid arthritis. *Immunol. Rev.* **233**, 233–255 (2010).

11. E. H. Noss, M. B. Brenner, The role and therapeutic implications of fibroblast-like synoviocytes in inflammation and cartilage erosion in rheumatoid arthritis. *Immunol. Rev.* **223**, 252–270 (2008).

12. D. S. Jones, A. P. Jenney, J. L. Swantek, J. M. Burke, D. A. Lauffenburger, P. K. Sorger, Profiling drugs for rheumatoid arthritis that inhibit synovial fibroblast activation. *Nat. Chem. Biol.* **13**, 38–45 (2017).

13. U. Müller-Ladner, J. Kriegsmann, B. N. Franklin, S. Matsumoto, T. Geiler, R. E. Gay, S. Gay, Synovial fibroblasts of patients with rheumatoid arthritis attach to and invade normal human cartilage when engrafted into SCID mice. *Am. J. Pathol.* **149**, 1607–1615 (1996).

14. S. Lefèvre, A. Knedla, C. Tennie, A. Kampmann, C. Wunrau, R. Dinser, A. Korb, E.-M. Schnäker, I. H. Tarner, P. D. Robbins, C. H. Evans, H. Stürz, J. Steinmeyer, S. Gay, J. Schölmerich, T. Pap, U. Müller-Ladner, E. Neumann, Synovial fibroblasts spread rheumatoid arthritis to unaffected joints. *Nat. Med.* **15**, 1414–1420 (2009).

15. T. Pap, K. R. Aupperle, S. Gay, G. S. Firestein, R. E. Gay, Invasiveness of synovial fibroblasts is regulated by p53 in the SCID mouse in vivo model of cartilage invasion. *Arthritis Rheum.* **44**, 676–681 (2001).

16. D. L. Scott, G. H. Kingsley, Tumor necrosis factor inhibitors for rheumatoid arthritis. *N. Engl. J. Med.* **355**, 704–712 (2006).

17. S. Cohen, E. Hurd, J. Cush, M. Schiff, M. E. Weinblatt, L. W. Moreland, J. Kremer, M. B. Bear, W. J. Rich, D. McCabe, Treatment of rheumatoid arthritis with anakinra, a recombinant human interleukin-1 receptor antagonist, in combination with methotrexate: Results of a twenty-four-week, multicenter, randomized, double-blind, placebo-controlled trial. *Arthritis Rheum.* **46**, 614–624 (2002).

18. S. B. Cohen, L. W. Moreland, J. J. Cush, M. W. Greenwald, S. Block, W. J. Shergy, P. S. Hanrahan, M. M. Kraishi, A. Patel, G. Sun, M. B. Bear; 990145 Study Group, A multicentre, double blind, randomised, placebo controlled trial of anakinra (Kineret), a recombinant interleukin 1 receptor antagonist, in patients with rheumatoid arthritis treated with background methotrexate. *Ann. Rheum. Dis.* **63**, 1062–1068 (2004).

19. R. N. Maini, P. C. Taylor, J. Szechinski, K. Pavelka, J. Bröll, G. Balint, P. Emery, F. Raemen, J. Petersen, J. Smolen, D. Thomson, T. Kishimoto, Double-blind randomized controlled clinical trial of the interleukin-6 receptor antagonist, tocilizumab, in European patients with rheumatoid arthritis who had an incomplete response to methotrexate. *Arthritis Rheum.* **54**, 2817–2829 (2006).

20. P. Emery, E. Keystone, H. P. Tony, A. Cantagrel, R. van Vollenhoven, A. Sanchez, E. Alecock, J. Lee, J. Kremer, IL-6 receptor inhibition with tocilizumab improves treatment outcomes in patients with rheumatoid arthritis refractory to anti-tumour necrosis factor biologicals: Results from a 24-week multicentre randomised placebo-controlled trial. *Ann. Rheum. Dis.* **67**, 1516–1523 (2008).

21. F. H. M. Prince, V. P. Bykerk, N. A. Shadick, B. Lu, J. Cui, M. Frits, C. K. Iannaccone, M. E. Weinblatt, D. H. Solomon, Sustained rheumatoid arthritis remission is uncommon in clinical practice. *Arthritis Res. Ther.* **14**, R68 (2012).

22. D. M. Schwartz, M. Bonelli, M. Gadina, J. J. O'Shea, Type I/II cytokines, JAKs, and new strategies for treating autoimmune diseases. *Nat. Rev. Rheumatol.* **12**, 25–36 (2016).

23. T. M. Lindstrom, W. H. Robinson, A multitude of kinases—Which are the best targets in treating rheumatoid arthritis? *Rheum. Dis. Clin. North Am.* **36**, 367–383 (2010).

24. M. C. Genovese, A. Kavanaugh, M. E. Weinblatt, C. Peterfy, J. DiCarlo, M. L. White, M. O'Brien, E. B. Grossbard, D. B. Magilavy, An oral Syk kinase inhibitor in the treatment of rheumatoid arthritis: A three-month randomized, placebo-controlled, phase II study in patients with active rheumatoid arthritis that did not respond to biologic agents. *Arthritis Rheum.* **63**, 337–345 (2011).

25. J. S. C. Arthur, S. C. Ley, Mitogen-activated protein kinases in innate immunity. *Nat. Rev. Immunol.* **13**, 679–692 (2013).

26. M. S. Hayden S Ghosh, NF-κB in immunobiology. *Cell Res.* **21**, 223–244 (2011).

27. T. Hanada, A. Yoshimura, Regulation of cytokine signaling and inflammation. *Cytokine Growth Factor Rev.* **13**, 413–421 (2002).

28. P. C. Taylor, M. Feldmann, Anti-TNF biologic agents: Still the therapy of choice for rheumatoid arthritis. *Nat. Rev. Rheumatol.* **5**, 578–582 (2009).

29. L. J. Gibbons, K. L. Hyrich, Biologic therapy for rheumatoid arthritis: Clinical efficacy and predictors of response. *BioDrugs* **23**, 111–124 (2009).

30. S.-S. Nah, H.-J. Won, E. Ha, I. Kang, H. Y. Cho, S.-J. Hur, S.-H. Lee, H. H. Baik, Epidermal growth factor increases prostaglandin E₂ production via ERK1/2 MAPK and NF-κB pathway in fibroblast like synoviocytes from patients with rheumatoid arthritis. *Rheumatol. Int.* **30**, 443–449 (2010).

31. M. Niepel, M. Hafner, E. A. Pace, M. Chung, D. H. Chai, L. Zhou, J. L. Muhlich, B. Schoeberl, P. K. Sorger, Analysis of growth factor signaling in genetically diverse breast cancer lines. *BMC Biol.* **12**, 20 (2014).

32. L. G. Alexopoulos, J. Saez-Rodriguez, B. D. Cosgrove, D. A. Lauffenburger, P. K. Sorger, Networks inferred from biochemical data reveal profound differences in toll-like receptor and inflammatory signaling between normal and transformed hepatocytes. *Mol. Cell. Proteomics* **9**, 1849–1865 (2010).

33. D. Duvenaud, D. Eaton, K. Murphy, M. Schmidt, Causal learning without DAGs. *J. Mach. Learn. Res. Workshop Conf. Proc.* **6**, 177–190 (2010).

34. Y. Benjamini, Y. Hochberg, Controlling the false discovery rate: A practical and powerful approach to multiple testing. *J. R. Stat. Soc. Series B Stat. Methodol.* **57**, 289–300 (1995).

35. H. Wajant, K. Pfizenmaier, P. Scheurich, Tumor necrosis factor signaling. *Cell Death Differ.* **10**, 45–65 (2003).

36. S. P. Davies, H. Reddy, M. Caivano, P. Cohen, Specificity and mechanism of action of some commonly used protein kinase inhibitors. *Biochem. J.* **351**, 95–105 (2000).

37. S. R. Selness, R. V. Devraj, B. Devadas, J. K. Walker, T. L. Boehm, R. C. Durley, H. Shieh, L. Xing, P. V. Rucker, K. D. Jerome, A. G. Benson, L. D. Marrufo, H. M. Madsen, J. Hitchcock, T. J. Owen, L. Christie, M. A. Promo, B. S. Hickory, E. Alvira, W. Naing, R. Blevis-Bal, D. Messing, J. Yang, M. K. Mao, G. Yalamanchili, R. Vonder Embse, J. Hirsch, M. Saabye, S. Bonar, E. Webb, G. Anderson, J. B. Monahan, Discovery of PH-797804, a highly selective and potent inhibitor of p38 MAP kinase. *Bioorg. Med. Chem. Lett.* **21**, 4066–4071 (2011).

38. A. de la Fuente, N. Bing, I. Hoeschele, P. Mendes, Discovery of meaningful associations in genomic data using partial correlation coefficients. *Bioinformatics* **20**, 3565–3574 (2004).

39. T. Zhang, F. Inesta-Vaquera, M. Niepel, J. Zhang, S. B. Ficarro, T. Machleidt, T. Xie, J. A. Marto, N. Kim, T. Sim, J. D. Laughlin, H. Park, P. V. LoGrasso, M. Patricelli, T. K. Nomanbhoy, P. K. Sorger, D. R. Alessi, N. S. Gray, Discovery of potent and selective covalent inhibitors of JNK. *Chem. Biol.* **19**, 140–154 (2012).

40. M. I. Davis, J. P. Hunt, S. Herrgard, P. Ciceri, L. M. Wodicka, G. Pallares, M. Hocker, D. K. Treiber, P. P. Zarrinkar, Comprehensive analysis of kinase inhibitor selectivity. *Nat. Biotechnol.* **29**, 1046–1051 (2011).

41. J. E. Overall, H. M. Rhoades, Beware of a half-tailed test. *Psychol. Bull.* **100**, 121–122 (1986).

42. R. A. Fisher, *Statistical Methods for Research Workers* (Oliver and Boyd, 1925).

43. M. R. Junttila, S.-P. Li, J. Westermarck, Phosphatase-mediated crosstalk between MAPK signaling pathways in the regulation of cell survival. *FASEB J.* **22**, 954–965 (2008).

44. D. Fey, D. R. Croucher, W. Kolch, B. N. Kholodenko, Crosstalk and signaling switches in mitogen-activated protein kinase cascades. *Front. Physiol* **3**, 355 (2012).

45. M. Fallahi-Sichani, N. J. Moerke, M. Niepel, T. Zhang, N. S. Gray, P. K. Sorger, Systematic analysis of BRAF^V600E melanomas reveals a role for JNK/c-Jun pathway in adaptive resistance to drug-induced apoptosis. *Mol. Syst. Biol.* **11**, 797 (2015).

46. C. J. Staples, D. M. Owens, J. V. Maier, A. C. B. Cato, S. M. Keyse, Cross-talk between the p38α and JNK MAPK pathways mediated by MAP kinase phosphatase-1 determines cellular sensitivity to UV radiation. *J. Biol. Chem.* **285**, 25928–25940 (2010).

47. C. Casals Casas, E. Álvarez, M. Serra, C. de la Torre, C. Farrera, E. Sánchez Tilló, C. Caelles, J. Lloberas, A. Celada, CREB and AP-1 activation regulates MKP-1 induction by LPS or M-CSF and their kinetics correlate with macrophage activation versus proliferation. *Eur. J. Immunol.* **39**, 1902–1913 (2009).

48. Y. Q. Xiao, K. Malcolm, G. S. Worthen, S. Gardai, W. P. Schiemann, V. A. Fadok, D. L. Bratton, P. M. Henson, Cross-talk between ERK and p38 MAPK mediates selective suppression of pro-inflammatory cytokines by transforming growth factor-β. *J. Biol. Chem.* **277**, 14884–14893 (2002).

49. G. Molina, A. Vogt, A. Bakan, W. Dai, P. Queiroz de Oliveira, W. Znosko, T. E. Smithgall, I. Bahar, J. S. Lazo, B. W. Day, M. Tsang, Zebrafish chemical screening reveals an inhibitor of Dusp6 that expands cardiac cell lineages. *Nat. Chem. Biol.* **5**, 680–687 (2009).

50. S. Naqvi, A. Macdonald, C. E. McCoy, J. Darragh, A. D. Reith, J. S. C. Arthur, Characterization of the cellular action of the MSK inhibitor SB-747651A. *Biochem. J.* **441**, 347–357 (2012).

51. M. Cargnello, P. P. Roux, Activation and function of the MAPKs and their substrates, the MAPK-activated protein kinases. *Microbiol. Mol. Biol. Rev.* **75**, 50–83 (2011).

52. P. Kahle, J. G. Saal, K. Schaudt, J. Zacher, P. Fritz, G. Pawelec, Determination of cytokines in synovial fluids: Correlation with diagnosis and histomorphological characteristics of synovial tissue. *Ann. Rheum. Dis.* **51**, 731–734 (1992).

53. S. J. Thomas, J. A. Snowden, M. P. Zeidler, S. J. Danson, The role of JAK/STAT signalling in the pathogenesis, prognosis and treatment of solid tumours. *Br. J. Cancer* **113**, 365–371 (2015).

54. M. J. Thiel, C. J. Schaefer, M. E. Lesch, J. L. Mobley, D. T. Dudley, H. Tecle, S. D. Barrett, D. J. Schrier, C. M. Flory, Central role of the MEK/ERK MAP kinase pathway in a mouse model of rheumatoid arthritis: Potential proinflammatory mechanisms. *Arthritis Rheum.* **56**, 3347–3357 (2007).

55. A. R. Brasier, The NF-κB regulatory network. *Cardiovasc. Toxicol.* **6**, 111–130 (2006).

56. C. Carmona-Rivera, P. M. Carlucci, E. Moore, N. Lingampalli, H. Uchtenhagen, E. James, Y. Liu, K. L. Bicker, H. Wahamaa, V. Hoffmann, A. I. Catrina, P. R. Thompson, J. H. Buckner, W. H. Robinson, D. A. Fox, M. J. Kaplan, Synovial fibroblast-neutrophil interactions promote pathogenic adaptive immunity in rheumatoid arthritis. *Sci. Immunol.* **2**, eaag3358 (2017).

57. N. J. Avdi, K. C. Malcolm, J. A. Nick, G. S. Worthen, A role for protein phosphatase-2A in p38 mitogen-activated protein kinase-mediated regulation of the c-Jun NH$_2$-terminal kinase pathway in human neutrophils. *J. Biol. Chem.* **277**, 40687–40696 (2002).

58. J. Westermarck, S.-P. Li, T. Kallunki, J. Han, V.-M. Kähäri, p38 mitogen-activated protein kinase-dependent activation of protein phosphatases 1 and 2A inhibits MEK1 and MEK2 activity and collagenase 1 (MMP-1) gene expression. *Mol. Cell. Biol.* **21**, 2373–2383 (2001).

59. P. C. F. Cheung, D. G. Campbell, A. R. Nebreda, P. Cohen, Feedback control of the protein kinase TAK1 by SAPK2a/p38α. *EMBO J.* **22**, 5793–5805 (2003).

60. M. Gaestel, A. Kotlyarov, M. Kracht, Targeting innate immunity protein kinase signalling in inflammation. *Nat. Rev. Drug Discov.* **8**, 480–499 (2009).

61. D. N. Krementsov, T. M. Thornton, C. Teuscher, M. Rincon, The emerging role of p38 mitogen-activated protein kinase in multiple sclerosis and its models. *Mol. Cell. Biol.* **33**, 3728–3734 (2013).

62. A. Ngkelo, I. M. Adcock, New treatments for COPD. *Curr. Opin. Pharmacol.* **13**, 362–369 (2013).

63. M.-J. Bertrand, J.-C. Tardif, Inflammation and beyond: New directions and emerging drugs for treating atherosclerosis. *Expert Opin. Emerg. Drugs* **22**, 1–26 (2017).

64. M. Fisk, P. R. Gajendragadkar, K. M. Mäki-Petäjä, I. B. Wilkinson, J. Cheriyan, Therapeutic potential of p38 MAP kinase inhibition in the management of cardiovascular disease. *Am. J. Cardiovasc. Drugs* **14**, 155–165 (2014).

65. S. Wang, L. Ding, H. Ji, Z. Xu, Q. Liu, Y. Zheng, The role of p38 MAPK in the development of diabetic cardiomyopathy. *Int. J. Mol. Sci.* **17**, 1037 (2016).

66. L. Leung, C. M. Cahill, TNF-α and neuropathic pain—A review. *J. Neuroinflammation* **7**, 27 (2010).

67. X. Lin, M. Wang, J. Zhang, R. Xu, p38 MAPK: A potential target of chronic pain. *Curr. Med. Chem.* **21**, 4405–4418 (2014).

68. S. Rosengren, D. L. Boyle, G. S. Firestein, Acquisition, culture, and phenotyping of synovial fibroblasts. *Methods Mol. Med.* **135**, 365–375 (2007).

69. Y. Benjamini, D. Yekutieli, The control of the false discovery rate in multiple testing under dependency. *Ann. Stat.* **4**, 1165–1188 (2001).

70. M. Mader, A. de Dios, C. Shih, R. Bonjouklian, T. Li, W. White, B. López de Uralde, C. Sánchez-Martinez, M. del Prado, C. Jaramillo, E. de Diego, L. M. Martín Cabrejas, C. Dominguez, C. Montero, T. Shepherd, R. Dally, J. E. Toth, A. Chatterjee, S. Pleite, J. Blanco-Urgoiti, L. Perez, M. Barberis, M. J. Lorite, E. Jambrina, C. R. Nevill, P. A. Lee, R. C. Schultz, J. A. Wolos, L. C. Li, R. M. Campbell, B. D. Anderson, Imidazolyl benzimidazoles and imidazo[4,5-b]pyridines as potent p38α MAP kinase inhibitors with excellent in vivo antiinflammatory properties. *Bioorg. Med. Chem. Lett.* **18**, 179–183 (2008).

71. D. M. Goldstein, A. Kuglstatter, Y. Lou, M. J. Soth, Selective p38α inhibitors clinically evaluated for the treatment of chronic inflammatory disorders. *J. Med. Chem.* **53**, 2345–2353 (2010).

72. C. Pargellis, L. Tong, L. Churchill, P. F. Cirillo, T. Gilmore, A. G. Graham, P. M. Grob, E. R. Hickey, N. Moss, S. Pav, J. Regan, Inhibition of p38 MAP kinase by utilizing a novel allosteric binding site. *Nat. Struct. Biol.* **9**, 268–272 (2002).

73. J. Regan, S. Breitfelder, P. Cirillo, T. Gilmore, A. G. Graham, E. Hickey, B. Klaus, J. Madwed, M. Moriak, N. Moss, C. Pargellis, S. Pav, A. Proto, A. Swinamer, L. Tong, C. Torcellini, Pyrazole urea-based inhibitors of p38 MAP kinase: From lead compound to clinical candidate. *J. Med. Chem.* **45**, 2994–3008 (2002).

74. E. R. Ottosen, M. D. Sørensen, F. Björkling, T. Skak-Nielsen, M. S. Fjording, H. Aaes, L. Binderup, Synthesis and structure-activity relationship of aminobenzophenones. A novel class of p38 MAP kinase inhibitors with high antiinflammatory activity. *J. Med. Chem.* **46**, 5651–5662 (2003).

75. P. S. Changelian, M. E. Flanagan, D. J. Ball, C. R. Kent, K. S. Magnuson, W. H. Martin, B. J. Rizzuti, P. S. Sawyer, B. D. Perry, W. H. Brissette, S. P. McCurdy, E. M. Kudlacz, M. J. Conklyn, E. A. Elliott, E. R. Koslov, M. B. Fisher, T. J. Strelevitz, K. Yoon, D. A. Whipple, J. Sun, M. J. Munchhof, J. L. Doty, J. M. Casavant, T. A. Blumenkopf, M. Hines, M. F. Brown, B. M. Lillie, C. Subramanyam, C. Shang-Poa, A. J. Milici, G. E. Beckius, J. D. Moyer, C. Su, T. G. Woodworth, A. S. Gaweco, C. R. Beals, B. H. Littman, D. A. Fisher, J. F. Smith, P. Zagouras, H. A. Magna, M. J. Saltarelli, K. S. Johnson, L. F. Nelms, S. G. Des Etages, L. S. Hayes, T. T. Kawabata, D. Finco-Kent, D. L. Baker, M. Larson, M.-S. Si, R. Paniagua, J. Higgins, B. Holm, B. Reitz, Y.-J. Zhou, R. E. Morris, J. J. O'Shea, D. C. Borie, Prevention of organ allograft rejection by a specific Janus kinase 3 inhibitor. *Science* **302**, 875–878 (2003).

Science Signaling

Inflammatory but not mitogenic contexts prime synovial fibroblasts for compensatory signaling responses to p38 inhibition

Douglas S. Jones, Anne P. Jenney, Brian A. Joughin, Peter K. Sorger and Douglas A. Lauffenburger

Context complicates network models

In rheumatoid arthritis (RA), inflammation is driven by the increased activity of the kinase p38 MAPK. However, p38 MAPK inhibitors are ineffective in patients. Using synovial fibroblasts and synovial fluid from RA patients, Jones *et al.* found that unlike cells in proliferative conditions, such as those in which cancer cells are grown (from which many network models have been built), p38 MAPK was a critical inducer of negative cross-talk to the MAPK-related, JNK pathway in cells grown in the inflammatory context associated with RA. Thus, inhibiting p38 facilitated JNK activity and the perpetuation of inflammatory cytokine production. Culturing the same cells under proliferative conditions switched the dominant point of negative cross-talk between the MAPK pathways to the kinase MEK. Inhibitors of the upstream kinase TAK1 curbed the activity of both the p38 and JNK pathways in the cells and, hence, might be effective in RA patients.

ARTICLE TOOLS	http://stke.sciencemag.org/content/11/520/eaal1601
SUPPLEMENTARY MATERIALS	http://stke.sciencemag.org/content/suppl/2018/03/02/11.520.eaal1601.DC1
RELATED CONTENT	http://stke.sciencemag.org/content/sigtrans/9/431/ra59.full http://stke.sciencemag.org/content/sigtrans/10/475/eaah4273.full http://stm.sciencemag.org/content/scitransmed/7/288/288ra76.full
REFERENCES	This article cites 74 articles, 17 of which you can access for free http://stke.sciencemag.org/content/11/520/eaal1601#BIBL
PERMISSIONS	http://www.sciencemag.org/help/reprints-and-permissions